SOIL SCIENCE SOCIETY OF AMERICA
JOURNAL

VOL. 52 MARCH-APRIL 1988 NO. 2

DIVISION S-1—SOIL PHYSICS

Hydraulic Conductivity of a Sandy Soil at Low Water Content After Compaction by Various Methods

JOHN R. NIMMO* AND KATHERINE C. AKSTIN

ABSTRACT

To investigate the degree to which compaction of a sandy soil influences its unsaturated hydraulic conductivity K, samples of Oakley sand (now in the Delhi series; mixed, thermic, Typic Xeropsamments) were packed to various densities and K was measured by the steady-state centrifuge method. The air-dry, machine packing was followed by centrifugal compression with the soil wet to about one-third saturation. Variations in (i) the impact frequency and (ii) the impact force during packing, and (iii) the amount of centrifugal force applied after packing, produced a range of porosity from 0.333 to 0.380. With volumetric water content θ between 0.06 and 0.12, K values were between 7×10^{-11} and 2×10^{-8} m/s. Comparisons of K at a single θ value for samples differing in porosity by about 3% showed as much as fivefold variation for samples prepared by different packing procedures, while there generally was negligible variation (within experimental error of 8%) where the porosity difference resulted from a difference in centrifugal force. Analysis involving capillary-theory models suggests that the differences in K can be related to differences in pore-space geometry inferred from water retention curves measured for the various samples.

Additional Index Words: **Bulk density, Porosity, Soil structure, Steady-state flow, Centrifuge, Soil-packing machines, Water retention, Capillary theory, Pore-space geometry.**

BOTH PRACTICAL and theoretical soil physics problems require knowledge of the effect of compaction on unsaturated hydraulic conductivity K. Besides the obvious application to water movement in porous media subjected to natural or artificial compaction, this issue is important wherever K is measured by techniques that involve compaction in sampling or sample preparation.

We use the term *compaction* to mean any change in the arrangement of particles that reduces the total volume of the medium, including simple compression and compaction associated with impacts. The comparison of K measurements at different degrees of compaction is best done for equal values of volumetric water content, θ, for which we use the notation K_θ. This mode of comparison partly compensates for pore-size changes; flow paths at the same θ have, on the average, the same cross-sectional dimensions.

Very little direct experimental evidence on the compaction dependence of K_θ is available. Several studies (Laliberte and Brooks, 1967; Douglas and McKyes, 1978; Lipiec and Tarkiewicz, 1986) considered the effect of packing density on K compared at equal values of matric potential ψ. The trend of K at equal θ values cannot be determined from these without knowledge of the $\theta(\psi)$ characteristics. A K_θ comparison is possible in the studies of Staple and Lehane (1954) and Koleva (1974), both of which used a K determination based on θ redistribution in soil columns after infiltration. In the cases where there was a clear and consistent trend, K_θ was greater in denser soil. The method used, however, is subject to systematic errors that may be responsible for this trend. Staple and Lehane acknowledged that additional work with improved methods would be necessary to establish a functional relationship between K and density.

Blake et al. (1976) observed significant $K(\theta)$ differences between compacted and uncompacted field plots that differed in bulk density by about 12%. The measurements were done on a clay loam at about 70% of saturation using a modified instantaneous profile method (Allmaras et al., 1975). K_θ in the compacted soil was less by a factor of 5 to 10.

In the absence of measurements, researchers have calculated expected compaction effects on $K(\theta)$ by applying capillary theory to measured values of $\theta(\psi)$ and saturated hydraulic conductivity K_{sat}. Typical $\theta(\psi)$ relations (e.g., Croney and Coleman, 1954) show greater water retention in the dry range and less in the wet

U.S. Geological Survey, Water Resources Div., 345 Middlefield Road, Menlo Park, CA 94025. Contribution from the U.S. Geological Surv., Menlo Park. Received 8 May 1987. *Corresponding author.

Published in Soil Sci. Soc. Am. J. 52:303–310 (1988).

range for denser soil. K_{sat} values normally increase with porosity ϕ, as commonly described by various empirical or partly empirical relations (Warkentin, 1971). When capillary theory models are used to predict $K(\theta)$ from these types of data, in general there is a strong increase of K_θ with porosity. Such a result was obtained by Reicosky et al. (1981), who applied Campbell's (1974) method to K_{sat} and $\theta(\psi)$ for a loam compacted to different bulk densities. The modeled K_θ differences increase with dryness of soil, becoming as great as several orders of magnitude. Similarly, Klein et al. (1983) applied the method of Green and Corey (1971) to $\theta(\psi)$ measurements from soils compressed at different water contents to the same final porosity. Their results also show K_θ values that differ by several orders of magnitude. The computed $K(\theta)$ curves are greater for soil compacted below, rather than above, the optimum water content (i.e., the water content at which the greatest compaction occurs for a given applied force). Because ϕ was the same for the two samples, these large predicted K_θ differences are based entirely on the difference in preparation technique.

Present knowledge suggests that K_θ differences due to compaction may be significant and that the critical structural differences may or may not be well correlated with ϕ. Direct experimental evidence is scarce, however. In particular, the theoretical predictions of very large K_θ differences in the dry range, which may have little relation to the more well known ϕ dependence of K at saturation, have not been tested. In the present study we attempt to accurately measure the influence of compaction on dry-range values of K compared at constant θ. We also investigate the effect of variations in method of compaction.

EXPERIMENT

Our basic experimental plan was to take soil from a large, thoroughly homogenized batch, pack it into columns by a means that permits easy adjustment of packed density, compact it further using centrifugal force, and then to measure K and ψ over a range of θ that overlaps for the various samples. For measuring $K(\theta)$ we use the steady-state centrifuge method (Nimmo et al., 1987). While the accuracy of this method permits small ($\pm 8\%$) differences in K_θ to be discerned, its speed makes it practical to obtain several measurements on each sample before aging effects become significant. The present state of development of this method makes its use easiest with coarse-textured media in a moisture range considerably drier than saturation.

The medium used in this study was Oakley sand, now classified in the Delhi series. The particle density of this soil was 2.737 Mg/m^3 and the specific surface, determined using a dynamic Brunauer-Emmett-Teller method (Flowsorb apparatus, Micromeritics, Norcross, GA),[1] was 4.2 m^2/g. The clay, silt, and sand fractions were 3.8, 3.6, and 92.6%. The sand fraction breaks down further as 13% coarse, 37% medium, 33% fine, and 9.6% very fine.

Soil columns were packed using the method and apparatus of Ripple et al. (1973). This technique is basically a dry deposition of soil with vertical-drop impacts and damping of subsidiary apparatus vibrations. A stack of as many as ten 4-cm-high, 5-cm-diam stainless steel sample retainers was packed at one time, requiring about 45 min. To produce samples with different bulk densities, we varied (i) the frequency of impacts by adjusting the rate of rotation of the cam that initiated impacts, and (ii) the magnitude of impacts by adjusting the height the column was allowed to fall before each impact. Table 1 gives the two values of impact frequency (F1 and F2) and drop height (D1 and D2) used in this study. These degrees of severity are within the ranges found by Ripple et al. (1973) to have no problems from radial particle-size segregation.

[1] Mention of specific brand names is for identification purposes only and does not imply endorsement by the U.S. Geological Survey.

Table 1. Three different means of influencing the porosity of packed samples and the two degrees of severity defined for each.†

Compacting influence	Degree 1	Degree 2
Drop height	0.6 mm (D1)	2.8 mm (D2)
Frequency of impacts	1/100 s (F1)	1/1.8 s (F2)
Centrifugation	140 g (C1)	1910 g (C2)

† The notations D1, D2, F1, etc., are used elsewhere in this paper to specify the preparation procedure used for a given sample.

Before measuring K by the steady-state centrifuge method, we precompacted the samples in the centrifuge as was done by Nimmo et al. (1987). In the first precompaction step, the samples start out being nearly saturated and are subjected to centrifugal force with no replenishment of soil water or additional mass placed on top of the soil. Water flows out during this step, leaving the samples at a water content of about 0.06 m^3 water/m^3. After rewetting, the samples were centrifuged for a few hours using the entire steady-state flow apparatus (Nimmo et al., 1987, Fig. 7). This apparatus includes the constant-head reservoir with ceramic applicator plate, weighing about 220 g, which rests on the top surface of the soil to exert a compressive force and produce flow sufficient to maintain a water content of about 0.09 m^3 water/m^3. Table 1 gives the values of centrifugal force (C1 and C2) used to achieve two degrees of compaction by centrifugation. The values refer to the force at the midpoint of the soil column, 19.0 cm from the axis of the centrifuge, at angular speeds of 84 and 314/s. Neglecting non-one-dimensional components of the centrifugal force and friction between the soil and the retainer walls, the pressure applied in a C1 compaction is equivalent to an overburden of about 130 kPa at the top of the sample, increasing to 230 kPa at the bottom. In a C2 compaction the equivalent overburden is 1800 kPa at the top of the sample and 3100 kPa at the bottom. Bulk density and porosity were determined from measurements of the sample volume and the known dry soil mass and particle density. Both C1 and C2 compactions produced samples whose density changed negligibly with further centrifugation at the 84/s speed used in K measurements.

The particular treatment used in preparing a given sample is specified by the combination of levels of severity of the following three adjustable influences: drop height, frequency of impacts, and centrifuge compaction. Individual packings are identified by the combination of D and F levels, the letters a and b being used to distinguish packings done at different times with the same choice of severity levels. Thus the full specification of a preparation procedure is given by such notation as D1F2aC2.

With most samples we obtained dual sets of K, θ, and ψ measurements, first after C1 compaction and again after C2 compaction. Details of the procedures are described by Nimmo et al. (1987). The volume occupied by the known mass of soil was measured to determine ϕ. Different water contents were obtained by applying water to the soil through porous plates made of different types of ceramic. As in the previous study, which also used Oakley sand, θ and ψ were essentially uniform within the samples once steady-state conditions were obtained. This meant that average θ measurements (computed from the sample weight) and single-point ψ measurements (obtained, when practical, with a tensiometer) were representative of the sample as a whole.

For some of the samples, we measured K_{sat} using constant-

Table 2. Measured porosity values (means with standard deviations) for Oakley sand resulting from combinations of packing type and centrifuge compaction.

Packing type	C0	C1	C2
D2F2	0.368 ± 0.003	0.347 ± 0.002	0.333 ± 0.001
D2F1	0.416 ± 0.001	0.369 ± 0.001	0.359 ± 0.001
D1F2	0.417 ± 0.007	0.380 ± 0.003	0.364 ± 0.003

head gravity-driven steady-state flow. Before saturating for this purpose, samples were drained in the centrifuge to θ values of about 0.04 m^3 water/m^3, and were then flushed with CO_2 to minimize entrapped air. The K_{sat} measurement was done only after all $K(\theta)$ measurements were complete for a given sample, because the required handling procedures prevent its reuse in an unsaturated state.

One limitation of the steady-state centrifuge method is that $K(\theta)$ measurements cannot be obtained for uncentrifuged (C0) samples, even though it would be useful to know how much $K(\theta)$ changes in the compaction from C0 to C1. For use in model calculation of $K(\theta)$, we made pressure-plate $\theta(\psi)$ measurements on C0 as well as C1 and C2 samples. These measurements spanned the ψ range from -8 to -50 kPa. The method used was a modification of the standard technique described by Richards (1965), involving 48 h of equilibration at each pressure step. The modification, to permit use of each sample at more than one pressure, was developed by C.D. Ripple and described by Stonestrom (unpublished laboratory procedure, 1980). It uses a small ceramic disk attached to the bottom of each sample and a diatomaceous earth pad to ensure good contact between this disk and the pressure plate. The 2-d pressure-plate method requires samples 1 cm high, but the centrifuge apparatus necessary for C1 and C2 compactions accepts only 4-cm-high samples. This led to difficulties in producing suitable samples that were equivalent to those used for $K(\theta)$ measurements. Instead of using the same stainless steel retainer as for $K(\theta)$, easily separated polypropylene rings were combined and 3-cm rings taped on top of 1-cm rings to give samples of the required size. Eight of these combinations, in addition to four single 1-cm rings for C0 measurements, were packed in a single D2F2 packing. Four of the combination retainers were compacted by the C1 procedure, and the other four by the C2 procedure. These samples were then drained using the centrifuge to θ of about 0.06 m^3 water/m^3, and the sections were separated. The 1-cm sections were used, along with the C0 samples, to obtain $\theta(\psi)$ data by the pressure-plate method. Differences between these samples and those used for $K(\theta)$ include: (i) a greater average compressive force on the 1-cm portion at the bottom of the stack, (ii) possibly nonequivalent centrifuge compaction in the less rigid polypropylene retainers, and (iii) the trimming of wet soil in the C0 samples. Another important distinction is that comparisons in this case involve different treatments applied to different samples, rather than different treatments successively applied to the same samples.

RESULTS

Table 2 indicates the final porosity values obtained for each type of sample preparation after steady-state centrifuge measurements of K and θ, and the initial (C0) porosities are given for comparison. Because good replication of porosities was obtained for (i) measurements done on the same sample at different times, (ii) measurements on different samples from the same packing, and (iii) measurements on samples from different packings with the same D and F levels, all three of these types of results were averaged.

Table 3 presents the results of the θ and ψ measurements done immediately after each steady-state K measurement. Experimental uncertainties for all measurements in this study were determined as by Nimmo et al. (1987), combining estimated measurement errors on each type of primary data. The combined random and systematic errors are ±2% for θ and ±3% for ψ. Averages were taken of any data points that fell within experimental error of each other. This averaging was necessary to permit interpolation by the modified-spline method of Stonestrom (1987) used in the model calculations described below. This method does not work when points are too close together.

Table 3. Water retention data obtained with the samples used for K measurements.

	C1		C2	
Packing	ψ (kPa)	θ	ψ (kPa)	θ
			−9.7	0.115
D2F2a	−9.4	0.116	−13.0	0.099
			−14.7	0.092
	−10.1	0.110	−17.5	0.090
			−27.0	0.081
D2F2b	−14.2	0.093		
	−15.2	0.089		
D2F1a	−9.7	0.113	−10.2	0.107
	−14.0	0.090	−14.0	0.094
	−21.0	0.078	−15.3	0.089
			−21.0	0.080
D1F2a	−6.8	0.092	−6.8	0.096
	−9.9	0.076	−9.4	0.080
	−16.8	0.063	−17.0	0.067
D1F2b	−9.4	0.104	−12.8	0.090
	−13.2	0.084	−13.4	0.085
			−14.0	0.083

Figures 1 to 4 show $K(\theta)$ for various preparations, grouped to illustrate the main features of the results. The point symbols in these graphs represent measurements; the experimental uncertainty for K is ±8%. The curves in Fig. 1 to 4, shown for illustrative purposes only, are computed from the empirical formula (cited, for example, by Hillel, 1980, p. 200)

$$K(\theta) = A\theta^n \quad [1]$$

where A and n are parameters determined by least-squares fits to the data.

Although several generalizations can be drawn from the $K(\theta)$ data set, one result stands out: the method of preparation is crucial. No single $K_\theta(\psi)$ function can describe the data. This fact is shown clearly in Fig. 1. Two of the three curves represent samples from the same (D2F1a) packing, differing only in centrifuge compaction, while the third is from the D1F2a packing. The two D2F1a curves are nearly identical. Even though the D1F2a curve corresponds to a sample porosity of 0.364, between the values 0.359 and 0.369 for the other two curves, it differs in K_θ by more than a factor of four. The three curves in Fig. 1 represent the major generalizations concerning the entire $K(\theta)$ data set.

Figure 2 shows the effect of variation in centrifuge compaction on $K(\theta)$. Though the porosity differs by about 0.015 (4% of the total porosity), there is relatively little difference in $K(\theta)$ for samples from the same packing compacted to different degrees by centrifugation. Of the four packings that can be compared in this way, the D1F2a case has the greatest difference in K_θ between the C1 and C2 treatments and the D2F2a case has the least. The D1F2a packing is the only such

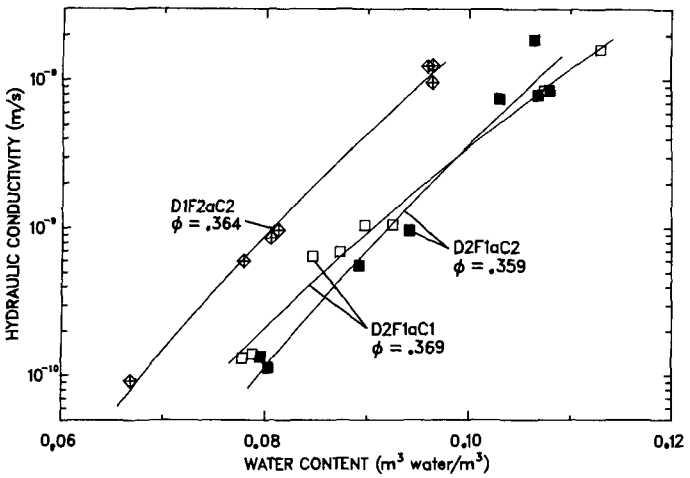

Fig. 1. Measured $K(\theta)$ data, comparing the effect of packing differences (D2F1aC2 vs. D1F2aC2) and centrifuge-compaction differences (D2F1aC2 vs. D2F1aC1).

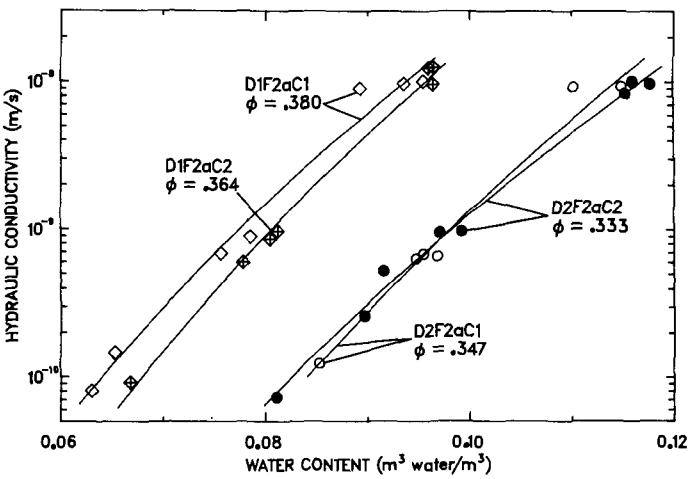

Fig. 2. Measured $K(\theta)$ data, showing the effects of C1 and C2 centrifuge compaction for the D1F2a and D2F2a packings.

case where the difference exceeds experimental error over the entire θ range. This difference, however, is small compared to the variation observed for different packings, even where ϕ values are close.

The next two figures show the entire $K(\theta)$ data set, C1 data in Fig. 3 and C2 data in Fig. 4. Of the eight D2F2aC2 data points in Fig. 4, five were previously reported by Nimmo et al. (1987). One of these points (at $\theta = 0.092$) represents 10 measurements with a mean of 5.22×10^{-10} m/s and a standard deviation 0.15×10^{-10} m/s. In both figures the $K(\theta)$ curves for different packings are markedly different, varying by a factor of 10 from the D2F2a to the D1F2a packings. The packings with greatest ϕ have greater K_θ than those with smallest ϕ. Although results were very consistent between samples from the same packing, there is poor agreement between replicate packings. This indicates a relevant but unknown and uncontrolled variable, perhaps the temperature or humidity of the packing room. The availability of 10 effectively identical samples from each packing permits adequate replication for the objectives of this study.

Figure 5 shows water retention data measured immediately after centrifuge K measurements for three different sample preparations. These data (from Table 3) were obtained using the same samples as for the $K(\theta)$ data in Fig. 1. The smooth curves connecting the points were determined as explained below in connection with model calculations. Clearly, the $\theta(\psi,\phi)$ data support the same basic generalizations as the $K(\theta,\phi)$ data: The curves are nearly identical for data from different degrees of centrifugation and are significantly different for different packings.

The pressure-plate water retention measurements [obtained with the 1-cm-high samples that were not used in $K(\theta)$ measurements] appear in Fig. 6. Of the four replicate samples of each preparatory treatment, two or three remained undamaged through the entire process and lead to successful $\theta(\psi)$ measurements, which were averaged to obtain the points in this graph. Here, in contrast to most of the $\theta(\psi)$ measurements for the samples used for $K(\theta)$, the difference between the C1 and C2 compactions exceeds experimental error. Figure 6 also shows a significant but smaller difference between the C0 and C1 data. When interpreting these results, it should be kept in mind that there were experimental difficulties in attempting to produce samples for pressure-plate measurements that were equivalent to those used for $K(\theta)$.

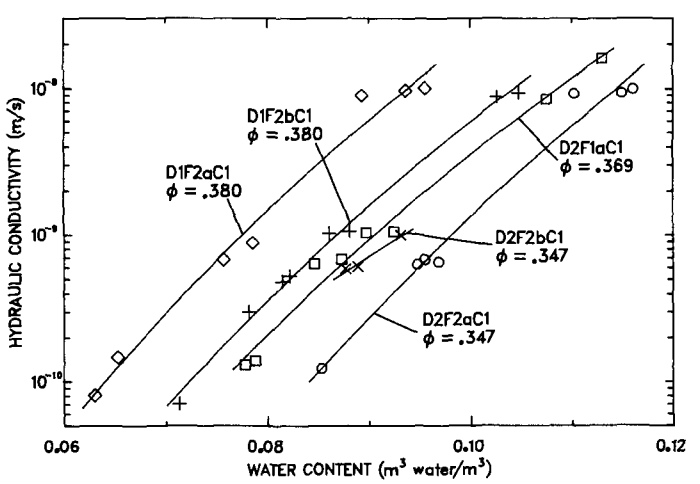

Fig. 3. Measured $K(\theta)$ data, showing the results of different packings subjected to C1 centrifuge compaction.

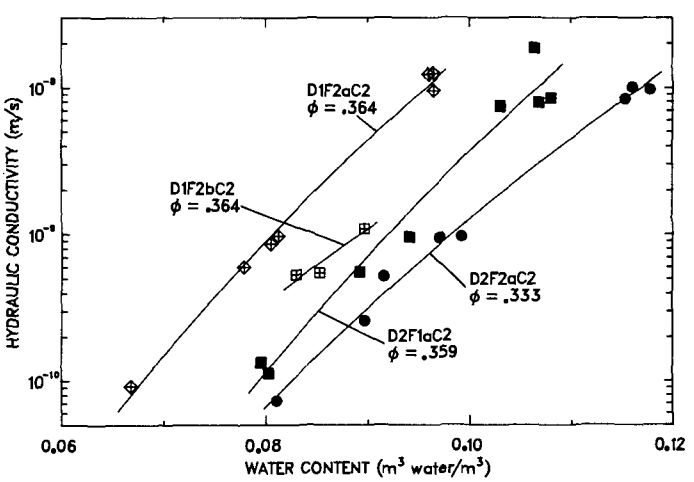

Fig. 4. Measured $K(\theta)$ data, showing the results of different packings subjected to C2 centrifuge compaction.

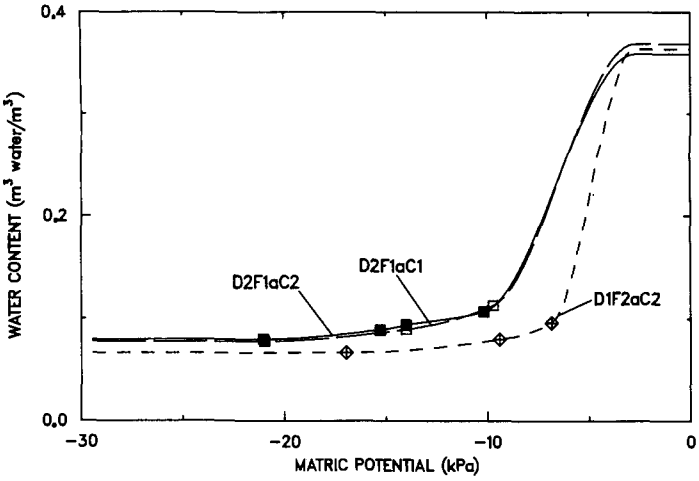

Fig. 5. Water retention data for the same samples for which $K(\theta)$ is shown in Fig. 1.

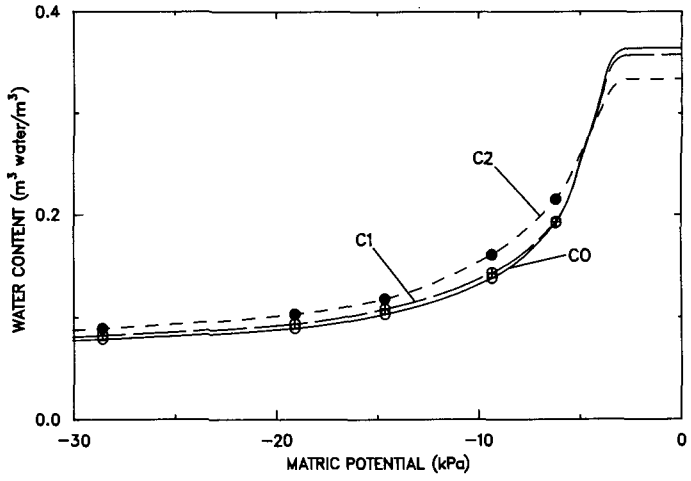

Fig. 6. Pressure-plate water-retention data for C0, C1, and C2 centrifuge compactions. All samples were from a single D2F2 packing.

Figure 7 shows the available K_{sat} measurements vs. ϕ. The experimental uncertainty for these K_{sat} values is ±6%. The solid curve is a fit to the Kozeny-Carman formula (Carman, 1956, p. 11–13).

$$K_{sat}(\phi) = B[\phi^3/(1 - \phi)^2] \quad [2]$$

in which the coefficient B was calculated by least-squares optimization to have a value of 4.389×10^{-4} m/s. The fact that the sensitivity of K_{sat} to ϕ only slightly exceeds that of the Kozeny-Carman relation is not surprising for a sandy medium. The dashed curve is a least-squares fit to the empirical formula

$$K_{sat}(\phi) = D_o \exp\left[D_1\left(\frac{\phi}{1 - \phi}\right)\right] \quad [3]$$

where D_0 and D_1 are parameters with the optimized values 5.142×10^{-7}m/s and 8.046. Equation [3] is a mathematical statement of the rule of thumb commonly used in soil mechanics (e.g., Taylor, 1948), that the logarithm of K_{sat} is linear with void ratio. The two-parameter formula [3] gives a reasonable fit for practical use (index of correlation 0.94).

To see whether K_{sat} shows the same dependence on preparation method as $K(\theta)$, C1 and C2 compactions for the same packing must be tested for near equality of K_{sat}. As mentioned previously, K_{sat} measurements could not be done on the same sample for C1 and C2 compactions, so samples from the same packing, with essentially identical $K(\theta)$, were used instead (the D1F2b points in Fig. 7). For these points there may be less variation in K_{sat} with ϕ, but the ±6% experimental error prevents a conclusive answer. The measured data do not contradict the hypothesis that for a sandy soil K_{sat} depends simply on porosity without regard to compaction method.

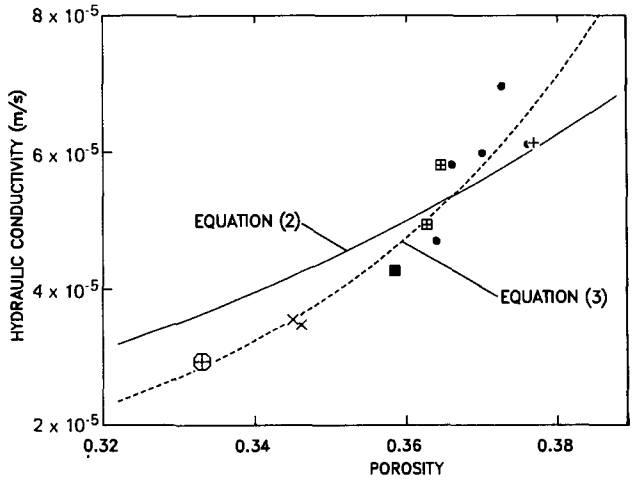

Fig. 7. Measurements of $K_{sat}(\phi)$ for Oakley sand. Those point symbols that are identical with those in Fig. 3 and 4 identify the preparation procedure by the same code. The point at $\phi = 0.333$ (cross in octagon) was determined with a D2F2C2 sample from a packing that preceded the D2F2a and D2F2b packings. The points indicated by small dots are from Stonestrom (1987).

MODEL CALCULATIONS

Because certain differences in compaction and preparation methods clearly affect both static and dynamic soil-moisture properties [$\theta(\psi)$ and $K(\theta)$], it is desirable to investigate a possible quantitative correlation between such effects on the two types of properties. One way of doing this is to use a model based on capillary theory. Four commonly applied models were tested:

1. The simple, straight, parallel tube model of Purcell (1949) as adapted for unsaturated media by Gates and Lietz (1950).
2. The simple tube model with a θ-dependent tortuosity factor (Burdine, 1953).
3. The original model of cut and rejoined tubes with smaller radius limiting flow (Childs and Collis-George, 1950).
4. The model of cut and rejoined tubes with pore lengths proportional to radii (Mualem, 1976).

The water retention data used with the capillary-theory models were taken from Table 3, so they were for exactly the same samples as the $K(\theta)$ values to be predicted. To formulate continuous $\theta(\psi)$ curves as shown in Fig. 5, interpolation and extrapolation methods were applied to the measured points in Table 3 and three additional fabricated points. Points (not explicitly shown in Fig. 5) were added at saturation ($\psi = 0$, $\theta = \phi$) and at the air-entry value ($\psi = -2.7$ kPa, $\theta = \phi$). The air-entry value was taken from mea-

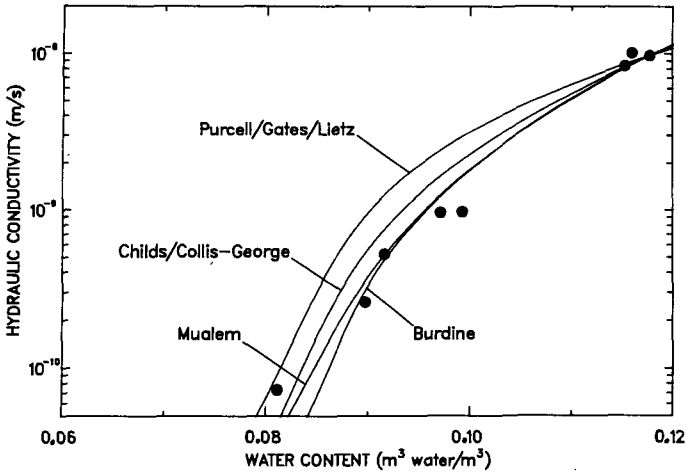

Fig. 8. $K(\theta)$ curves calculated using four different capillary-theory models for the D2F2aC2 data.

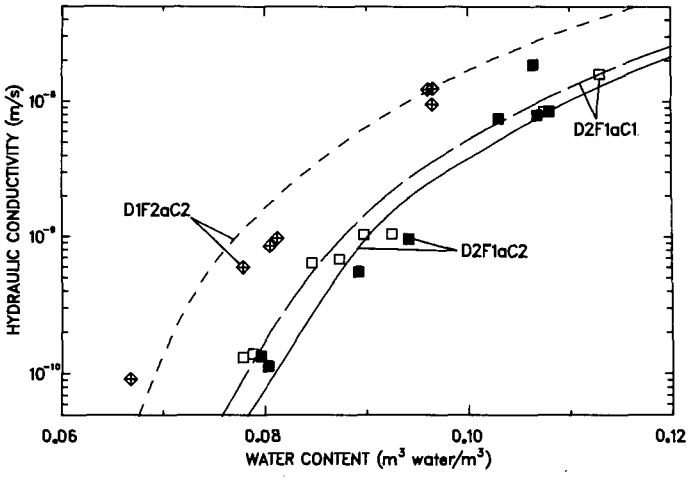

Fig. 9. $K(\theta)$ data of Fig. 1 with curves computed using the Mualem model and $\theta(\psi)$ data of Fig. 5 with matching factors determined by the wettest measured point on each curve.

surements by Stonestrom (1987) for the same batch of Oakley sand. The same value was used for all samples. This is reasonable because the air-entry value has no significant influence on model calculations in the range of interest and because the evidence of Laliberte and Brooks (1967) indicates air-entry values not to be very sensitive to soil compaction. Another point was added at $\psi = -1500$ kPa, based on measurements for Oakley sand (Ripple and Stonestrom, 1974, unpublished data) and the rule of thumb cited by Gardner (1968) that at -1500 kPa water is spread in a nearly uniform layer over the entire solid surface of the medium. For samples compacted differently, this assumption allows the calculation of θ using the formula

$$\theta(\phi,\psi_o) = \theta_o[(1 - \phi)/(1 - \phi_o)] \quad [4]$$

where θ_o is the known water content at matric potential ψ_o for the soil when its porosity is ϕ_o. Equation [4] is based on a direct proportionality between θ and surface area per unit volume, assuming that ψ alone determines the water layer thickness. Extrapolation to $\psi = -\infty$ was done using Brooks and Corey's (1964) formula, fit exactly to the -1500 kPa point and the driest measured point. Interpolation was done using Stonestrom's (1987) modified spline method, with slope matched to that of the Brooks and Corey curve at the -1500-kPa point and to a slope of zero at the air-entry value. Residual water content was taken to be zero in all model calculations.

Some effort was required to investigate the adequacy of the sparse data set and the extrapolations applied to the $\theta(\psi)$ curves. Because, according to capillary theory, the largest filled pores have the dominant influence on K at any given θ, the $\theta(\psi)$ measurements of greatest importance are those in the range for which K is to be modeled. Below this range the data correspond to very small pore sizes that minimally influence K computations and above it the data correspond to unfilled pores that have no influence on the computed K values. The sensitivity of model calculations to the estimated value of θ at -1500 kPa was tested and found to be slight. Calculations done after decreasing this value by half changed the modeled K at the driest measured point by only 15%. Similar tests were done on the θ values of the measured points to see whether each $\theta(\psi)$ measurement was essential. These tests showed the computed results to be very sensitive even to the driest of the measured data points. These sensitivity calculations established minimum data requirements for the generation of $\theta(\psi)$ curves suitable for model calculations: at least three measured $\theta(\psi)$ points spanning the range of $K(\theta)$ measurement in addition to the -1500-kPa and air-entry points.

Figure 8 shows how the four different models fit the D2F2aC2 data. The computations involved a matching factor based on the greatest measured $K(\theta)$, so each modeled curve goes through this point exactly. (The more common technique of matching at K_{sat} is less appropriate because the value of K_{sat} is more than three orders of magnitude greater.) Except for the simplest straight-tube (Purcell) model, the fits to the data are reasonable. Although the curvature of the modeled curves is not exactly as indicated by the data, the overall log-K-vs.-θ slope is in fair agreement. Judged by eye, the Mualem model provides the best fit.

In Fig. 9, Mualem model calculations based on the $\theta(\psi)$ curves of Fig. 5 agree very well with the slope, spacing, and absolute positions of the $K(\theta)$ measurements. As in Fig. 8, individual matching factors were determined using the wettest measured $K(\theta)$ point of each curve. Thus it is mainly significant that the overall slope and curvature are in reasonable agreement; these results are not a complete test of the model's agreement with experiment because the matching technique forced a perfect fit at one end of the curves.

Figure 10 illustrates a much stronger test of the Mualem model. Here, a single matching factor, determined for the D2F2aC2 data set, was used in computing all three curves. Even though none of the $K(\theta)$ data shown played a role in the calculations, the agreement is almost as good as in Fig. 9. Considering the data shown in Fig. 5, the fact that the relative spacing of the curves for different preparations reflects that of the $\theta(\psi)$ curves is not surprising, but for the actual positions of the curves to be in such good agreement with the data is significant. In applying this test to data for the other sample treatments, it was found that this

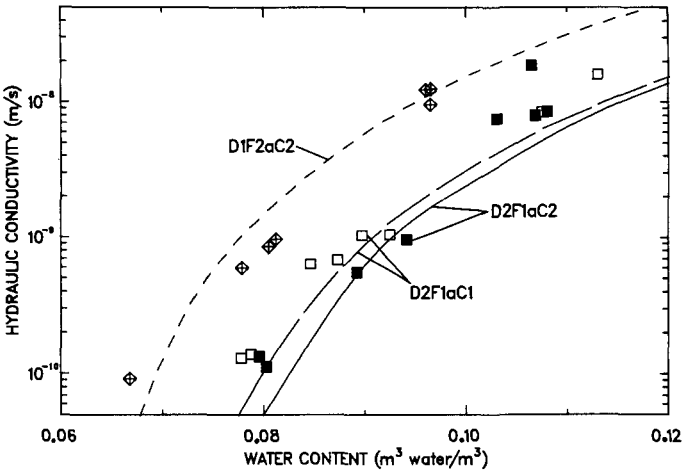

Fig. 10. $K(\theta)$ data of Fig. 1 with curves computed using the Mualem model and $\theta(\psi)$ data of Fig. 5 with a single matching factor determined for the D2F2aC2 data.

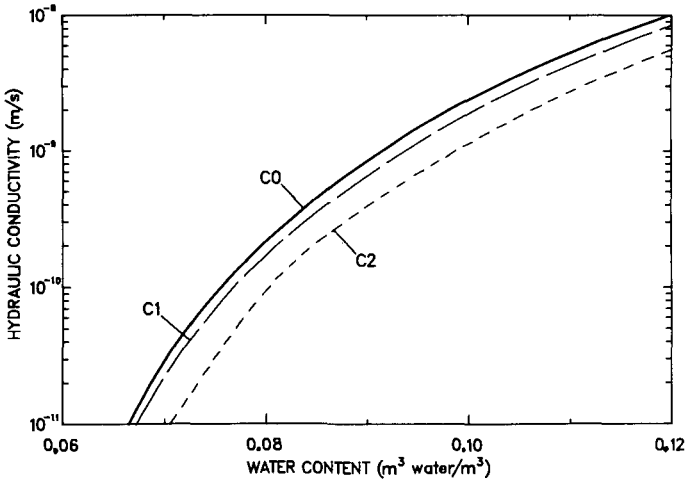

Fig. 11. $K(\theta)$ curves computed by the Mualem model for the C0, C1, and C2 data of Fig. 6, using the matching factor determined for the D2F2aC2 data.

same matching factor produced reasonable agreement between measurements and model calculations in all cases. Thus it appears that only one matching factor is needed to characterize a medium like Oakley sand in this moisture range.

The result that $\theta(\psi)$ data plus a single matching factor can effectively predict $K(\theta)$ measurements encouraged the application of the model to the pressure-plate data of Fig. 6. Of primary interest here is the effect on K of C1 compaction compared to uncentrifuged (C0) samples. The graphed results of this calculation in Fig. 11 indicate significant differences in K between all treatments. This result should only be interpreted in light of the difficulties of sample duplication discussed in connection with the Fig. 6 data. Even so, the 20% reduction of K_θ in going from C0 to C1 compaction may represent an upper limit on this effect, and is small compared to the differences observed for different packing procedures.

DISCUSSION

The chief questions raised by the data in this paper are (i) why the effect of variation in centrifuge compaction on K_θ is small, and (ii) why the effect of variation in machine packing is large. One type of important supplementary evidence is the K_{sat} measurements, which show a porosity dependence without regard to treatment. Another is the capillary-theory correlation between $\theta(\psi)$ and $K(\theta)$ results. This correlation means that where a compacted sample has fewer large pores and more small pores, as inferred from $\theta(\psi)$, its conductivity is reduced accordingly.

It is clear from Fig. 1 and 2 that even where centrifuge compaction is great enough to cause significant porosity changes, its influence on K_θ may be negligible. The resulting disruption of pore structure is small enough that critical differences originating in the various packing procedures are preserved. This result appears to contrast with the behavior observed at and near saturation. Figure 7, for example, shows a porosity dependence of K_{sat} independent of compaction method, and results of Blake et al. (1976) show a strong effect of compressive compaction near saturation. Considering the difference in water content, all of these results are consistent with the hypothesis that compressive compaction primarily affects large pores, those that are essentially empty for a sandy soil at <35% of saturation. It is plausible that the compression acts on an interlocked network of sand grains, reducing the large pores that dominate at and near saturation, while leaving the smallest pores essentially unchanged.

The great influence of machine packing on K_θ in this study indicates that even in a sandy medium, dry-deposition packing can strongly affect the small pores. The model agreement (e.g., Fig. 10) means that the soil has an element in common with a set of variably sized, cut-and-rejoined capillary tubes. The likely critical feature is that within capillary tubes, flow is confined in all directions perpendicular to the flow direction, and so is determined to a large degree by the size of the channels. In a filled, confined pore there are at least two influences that cause great sensitivity of flow resistance to structural change: (i) water is subject to viscous friction from all of the nearby confining surfaces, and (ii) any dimensional alteration of such a pore directly changes the size of the water-filled flow channel. In a capillary this sensitivity is evident in the inverse-fourth-power-of-radius dependence of flow rate in Poiseuille's law. On the other hand, for water in layers coating particle surfaces, in shallow crevices, or in other situations where it is unconstrained in at least one direction perpendicular to the flow direction, the sensitivity to the geometrical configuration of the particles is considerably less. As an example, it can be estimated what K_θ difference would result from the maximum porosity difference of this study, 0.380 to 0.333, assuming all flow is in uniform layers. Laminar flow theory (e.g., Bird et al., 1960, p. 37–40) applied to the assumptions of Eq. [4] indicates a scaling of K_θ according to

$$K(\phi,\theta_o) = K_o\,[(1 - \phi_o)^2/(1 - \phi)^2] \qquad [5]$$

where K_o is the known conductivity at water content θ_o for porosity ϕ_o. The resulting prediction is for K_θ differences of only 16%. This contrasts sharply with the measured K_θ differences of as much as one order of magnitude in Oakley sand. Therefore, even for the low-clay-content, low-θ conditions of this experiment,

flow must occur primarily in confined channels.

The size of the dominant flow channels is surprisingly small for a sandy soil. At ψ values of about -8 kPa, the largest filled pores would have an equivalent capillary radius of 15 μm. Thus the size and configuration of flow channels are probably determined largely by silt and clay particles rather than the framework of sand grains. If a "coating" of such particles constitutes the part of the medium (about 7% of total volume) within which most of the flow takes place, the situation becomes analogous to saturated flow through a fine-textured medium. Work done on this topic shows a strong dependence of K_{sat} on compaction, and in particular, on the water content of the medium at the time of compaction (e.g., Cary et al., 1943; Lambe, 1958b; Mitchell et al., 1965). Structural changes proposed to account for such effects (Lambe, 1958a; Diamond, 1971) may play a similar role in the fine-textured fraction of Oakley sand.

The mechanism through which subtle differences in the packing process affect $K(\theta)$ and $\theta(\psi)$ is hard to identify. One concern is that there may be a significant effect of changes in the temperature or humidity of the room in which packing takes place. Another is that varying amounts of fine particles may be lost as airborne dust, though such an effect would cause retention curves to become steeper rather than flatter, as observed. It is more likely that particles are oriented or arranged differently in the different packings. During deposition, particles are relatively free to rotate and move around with each impact. This is especially true for the vertical-drop method because the whole soil column is in free-fall just before each impact. The denser packings have particles more efficiently arranged in the available space, probably with more of the relatively flat surfaces in nearly parallel contact.

The results of this study are consistent with the hypothesis that sandy soil consists of an interlocked network of sand grains coated with a fine-textured medium. Centrifuge compaction may only compress the sand-grain framework, reducing ϕ and K_{sat} but leaving the fine-textured portion and, hence, the low-θ moisture properties, essentially unchanged. Compaction during packing apparently causes a significant disruption of the fine-textured portion, thereby strongly influencing $K(\theta)$ and $\theta(\psi)$ as well as ϕ and K_{sat}. Either bringing the fine particles closer together, or altering their orientation in a way that affects pore-size distribution, could cause an increase in water retention and a decrease in $K(\theta)$.

REFERENCES

Allmaras, R.R., W.W. Nelson, and W.B. Voorhees. 1975. Soybean and corn rooting in southwestern Minnesota I. Water uptake sink. Soil Sci. Soc. Am. Proc. 39:764–771.

Bird, R.B., W.E. Stewart, and E.N. Lightfoot. 1960. Transport phenomena. John Wiley & Sons, Inc., New York.

Blake, G.R., W.W. Nelson, and R.R. Allmaras. 1976. Persistence of subsoil compaction in a Mollisol. Soil Sci. Soc. Am. J. 40:943–948.

Brooks, R.H., and A.T. Corey. 1964. Hydraulic properties of porous media. Hydrology Paper no. 3. Colorado State Univ., Fort Collins.

Burdine, N.T. 1953. Relative permeability calculation from pore size distribution data. Trans. Am. Inst. Min. Metall. Eng. 198:71–78.

Campbell, G.S. 1974. A simple method for determining unsaturated conductivity from moisture retention data. Soil Sci. 117:311–314.

Carman, P.C. 1956. Flow of gases through porous media. Butterworths, London.

Cary, A.S., B.H. Walter, and H.T. Howard. 1943. Permeability of mud mountain dam core material. Trans. Am. Soc. Civ. Eng. 108:719–737.

Childs, E.C., and N. Collis-George. 1950. The permeability of porous materials. Proc. R. Soc. (London) 201A:392–405.

Croney, D., and J.D. Coleman. 1954. Soil structure in relation to soil suction (pF). J. Soil Sci. 5:75–84.

Diamond, S. 1971. Microstructure and pore structure of impact-compacted clays. Clays Clay Miner. 19:239–249.

Douglas, E., and E. McKyes, (1978). Compaction effects on the hydraulic conductivity of a clay soil. Soil Sci. 125:278–282.

Gardner, W.R. 1968. Availability and measurement of soil water. p. 107–135. *In* T.T. Kozlowski (ed.) Water and deficits and plant growth. Vol. I. Academic Press, New York.

Gates, J.I., and W. Tempelaar Lietz. 1950. Relative permeabilities of California cores by the capillary-pressure method. p. 285–298. *In* Drilling and production practice. Am. Petrol. Inst., New York.

Green, R.E., and J.C. Corey. 1971. Calculation of hydraulic conductivity: A further evaluation of some predictive methods. Soil Sci. Soc. Am. Proc. 35:3–8.

Hillel, D. 1980. Fundamentals of soil physics. Academic Press, New York.

Klein, S., T.M. Johnson, and K. Cartwright. 1983. Moisture characteristics of compacted soils for use in trench covers. p. 101–111. *In* J.W. Mercer et al. (ed.) Role of the unsaturated zone in radioactive and hazardous waste disposal. Ann Arbor Science, Ann Arbor, MI.

Koleva, S. 1974. Dependence of hydraulic conductivity on the moisture content and moisture potential at varying soil compaction. "Vodno Stopanstvo", Bulgaria. Pochvozn. Agrokhim. 9(6):31–41.

Laliberte, G.E., and R.H. Brooks. 1967. Hydraulic properties of disturbed soil materials affected by porosity. Soil Sci. Soc. Am. Proc. 31:451–454.

Lambe, T.W. 1958a. The structure of compacted clay. J. Soil Mech. Found. Div. Am. Soc. Civ. Eng. 84(SM2):1654.

Lambe, T.W. 1958b. The engineering behavior of compacted clay. J. Soil. Mech. Found. Div. Am. Soc. Civ. Eng. 84(SM2):1655.

Lipiec, J., and S. Tarkiewicz. 1986. The effect of soil compaction on the coefficient of hydraulic conductivity. Pol. J. Soil Sci. 17:9–14.

Mitchell, J.K., D.R. Hooper, and R.G. Campanella. 1965. Permeability of compacted clay. J. Soil Mech. Found. Div. Am. Soc. Civ. Eng. 91(SM4):41–65.

Mualem, Y. 1976. A new model for predicting the hydraulic conductivity of unsaturated porous media. Water Resour. Res. 12:513–522.

Nimmo, J.R, J. Rubin, and D.P. Hammermeister. 1987. Unsaturated flow in a centrifugal field: Measurement of hydraulic conductivity and testing of Darcy's law. Water Resour. Res. 23:124–134.

Purcell, W.R. 1949. Capillary pressures—their measurement using mercury and the calculation of permeability therefrom. Trans. Am. Inst. Min. Metall. Eng. 186:39–46.

Reicosky, D.C., W.B. Voorhees, and J.K. Radke. 1981. Unsaturated water flow through a simulated wheel track. Soil Sci. Soc. Am. J. 45:3–8.

Richards, L.A. 1965. Physical condition of water in soil. *In* C.A. Black et al. (ed.) Methods of soil analysis. Part 1. Agronomy 9:128–152.

Ripple, C.D., R.V. James, and J. Rubin. 1973. Radial particle-size segregation during packing of particulates into cylindrical containers. Powder Technol. 8:165–175.

Staple, W.J. and J.J. Lehane. 1954. Movement of moisture in unsaturated soils. Can. J. Agric. Sci. 34:329–342.

Stonestrom, D.A. 1987. Co-determination and comparisons of hysteresis-affected, parametric functions of unsaturated flow: Water-content dependence of matric pressure, air-trapping, and fluid permeabilities in a non-swelling soil. Ph.D. diss. Stanford Univ., Stanford, CA.

Taylor, D.W. 1948. Fundamentals of soil mechanics. John Wiley & Sons, New York.

Warkentin, B.P. 1971. Effects of compaction on content and transmission of water in soils. p. 126–221. *In* K.K. Barnes et al. (ed.) Compaction of agricultural soils. Am. Soc. of Agric. Eng., St. Joseph, MI.